

This is a provisional PDF only. Copyedited and fully formatted version will be made available soon.



**ISSN:** 0015-5659

**e-ISSN:** 1644-3284

## **Quantitative anatomy of the growing psoas major muscle in the human fetus – an anatomical, digital and statistical study**

**Authors:** Magdalena Grzonkowska, Michał Szpinda, Michał Kułakowski, Bartłomiej Hankiewicz, Karol Elster, Mariusz Baumgart

**DOI:** 10.5603/fm.104111

**Article type:** Original article

**Submitted:** 2024-12-18

**Accepted:** 2025-01-16

**Published online:** 2025-01-22

This article has been peer reviewed and published immediately upon acceptance. It is an open access article, which means that it can be downloaded, printed, and distributed freely, provided the work is properly cited.

Articles in "Folia Morphologica" are listed in PubMed.

## ORIGINAL ARTICLE

DOI: 10.5603/fm.104111

Magdalena Grzonkowska et al., Fetal psoas major muscle growth dynamics

### **Quantitative anatomy of the growing psoas major muscle in the human fetus — an anatomical, digital and statistical study**

Magdalena Grzonkowska<sup>1</sup>, Michał Szpinda<sup>2</sup>, Michał Kułakowski<sup>3</sup>, Bartłomiej Hankiewicz<sup>3</sup>, Karol Elster<sup>3</sup>, Mariusz Baumgart<sup>1</sup>

<sup>1</sup>Department of Normal Anatomy, the Ludwik Rydygier *Collegium Medicum* in Bydgoszcz, the Nicolaus Copernicus University in Toruń, Poland

<sup>2</sup>Bydgoszcz University of Science and Technology, Faculty of Medicine, Bydgoszcz, Poland

<sup>3</sup>Clinical Department of Orthopedics and Traumatology, Jan Biziel University hospital no. 2 in Bydgoszcz, Nicolaus Copernicus University in Toruń, Poland

**Address for correspondence:** Magdalena Grzonkowska, MD, Department of Normal Anatomy, the Ludwik Rydygier *Collegium Medicum* in Bydgoszcz, ul. Łukasiewicza 1, Bydgoszcz 85–821, Poland; tel. + 48 052 5853705, e-mail: [m.grzonkowska@cm.umk.pl](mailto:m.grzonkowska@cm.umk.pl)

## **ABSTRACT**

**Background:** In the present study we aimed to quantitatively evaluate the growth of the psoas major in human fetuses.

**Materials and methods:** Using anatomical dissection, digital-image analysis (NIS Elements AR 3.0), volumetric hydrostatic method, and statistical analysis (Student's *t*-test, regression analysis), the 10 direct morphometric parameters (4 lengths, 2 widths, 3 projection surface areas, and volume) of the psoas major were evaluated, and then the 5 morphometric indexes (belly width-to-length ratio, tendon width-to-length ratio, belly-to-muscle projection surface area ratio, tendon-to-muscle projection surface area ratio, and tendon-to-belly projection surface area ratio) were calculated in 67 human fetuses of both sexes (31 ♂, 36 ♀) aged 16–28 weeks.

**Results:** Neither male-female nor right-left significant differences were found in relation to numerical data of the growing psoas major. Both the total muscle length and tendon length increased logarithmically, the belly length followed the third-degree polynomial function, both the maximal belly width and midway tendon width followed inverse functions, while the distance from the muscle origin to the widest part of the muscle belly, 3 (muscle, belly and tendon) projection surface areas, and volume increased commensurately to fetal age.

**Conclusions:** In terms of morphometric parameters, the psoas major displays growth dynamics diverse to four functions: from a gradual inhibition of growth which is typical of both natural logarithmic functions (total length and tendon length) and a reverse model (belly width and tendon width) through a linear growth (distance between the origin and the widest belly level, muscle projection surface area, belly projection surface area, tendon projection surface area, and volume) to a hyperbolic growth (belly length).

**Keywords:** psoas major, human fetuses, fetal development

## INTRODUCTION

The psoas major muscle is one of the most important muscles in the human body. Due to its anatomical location, it is associated with an astonishing range of problems, including lower back pain [2, 8, 19, 24], sacroiliac pain [34], disc herniation [7, 24, 34], hip degeneration [25]. Additionally, the psoas major contributes to biomechanical issues such as pelvic tilt [14], leg length discrepancies [14], and lumbar lordosis [25, 34].

Between the superficial and deep layers of the psoas major lies the lumbar plexus. Due to the relatively underdeveloped state of the muscular system in fetuses, damage to the lumbar plexus can occur even during the intrauterine growth or delivery. It is important to emphasize that the iliopsoas muscle plays a protective role for the lumbar plexus; therefore, pathological changes within this muscle could have a detrimental impact on delicate nerve structures [26, 37]. In their study on the lumbar plexus in human fetuses, Yasar et al. [37] suggested during intrauterine growth, the ilioinguinal and iliohypogastric nerves are particularly delicate and susceptible to injury.

Developmental abnormalities of skeletal muscles can result to congenital defects that may occur in isolation or in combination with other anomalies, forming distinct pathological syndromes [14]. Prenatal imaging offers critical information of highly relevant for genetic counseling, monitoring fetal development, and implementing early in utero treatments [18, 22, 37].

Upon reviewing original morphometric studies of the psoas major, we were unable to identify any numerical data specifically referring to the fetal psoas major. Instead, using various imaging modalities such as ultrasonography (US) [27, 28], magnetic resonance imaging (MRI) [1, 2, 22], computed tomography (CT) [8, 16] and autopsy [14, 38], the psoas major has been thoroughly visualized and evaluated in adult individuals. Therefore, this study represents the first report in the medical literature to precisely analyze morphometric parameters of the psoas major muscle in the human fetus.

The objectives of the present study were as follows:

- to perform a comprehensive morphometric analysis of the psoas major muscle, including its linear, planar, and volumetric parameters, in order to establish age-specific reference values;
- to evaluate potential sex- and side-related differences in the analyzed parameters;
- to model the growth dynamics of the examined parameters using mathematical models that best correspond to fetal age.

## **MATERIALS AND METHODS**

The study material consisted of 67 fetuses of both sexes (31 males and 36 females) aged 16 to 28 weeks, obtained from spontaneous miscarriages and preterm deliveries. All fetuses were acquired prior to the year 2000 and remain part of the specimen collection in the Department of Normal Anatomy. It is noteworthy that the present experiment was approved by the Bioethics Committee of our University (KB 124/2016). Fetal age was determined based on crown-rump length measurements. Table 1 provides an overview of the study group, including fetal age, number and sex.

All fetuses were preserved through immersion in 10% neutral formalin solution. Functionally, formalin-fixed skeletal muscles exist in a state of partial contraction, intermediate between the fully relaxed and fully contracted states observed in living individuals [21]. It is noteworthy that a significant decrease in muscle length is typically observed when isolated muscles are subjected to fixation. This contrasts with our study, in which skeletal musculature was fixed *in situ*, i.e., attached to the skeleton [6].

Each psoas major muscle was anatomically dissected to fully visualize its course from origin to insertion, and was documented using a camera of Canon EOS 70D(W) (Canon, Tokyo, Japan) with a millimeter scale. Digital images of the psoas major were quantitatively analyzed using digital-image analysis software (NIS Elements AR 3.0; Nikon Instruments Inc., Tokyo, Japan), which semi-automatically estimated all the studied parameters (Fig. 1 A,

B). The digital method allowed for precise measurements with an accuracy of 0.1 mm. No fetal malformations or abnormalities of the psoas major muscle were identified, allowing the sample to be classified as normal. For each psoas major, 10 direct measurements (parameters 1–10) and 5 calculated values (parameters 11–15) were obtained (Fig. 1D):

1. total length — distance between the origin and insertion of the muscle (mm);
2. belly length — measured from its origin to its termination (mm);
3. tendon length — measured from its origin to its termination (mm);
4. distance between the muscle origin and the widest part of the muscle belly (mm);
5. belly width — measured at its widest level (mm);
6. tendon width — measured at its midway (mm);
7. muscle projection surface area — based on the contour of the whole muscle projection (mm<sup>2</sup>);
8. belly projection surface area — based on the contour of the muscle belly projection (mm<sup>2</sup>);
9. tendon projection surface area — based on the contour of the tendon projection (mm<sup>2</sup>);
10. muscle volume — using the hydrostatic method (mm<sup>3</sup>);
11. belly width-to-length ratio;
12. tendon width-to-length ratio;
13. belly-to-muscle projection surface area ratio;
14. tendon-to-muscle projection surface area ratio;
15. tendon-to-belly projection surface area ratio.

Notably, the volumetric method was based on Archimedes' principle and involved a double weighing procedure, measuring the psoas major both in air and in distilled water (Fig. 1C). For each muscle, the double-weighing procedure was repeated three times. To accurately determine the volume of the psoas major muscle, the following formula was applied:

$$V = \frac{\Delta m - 0.001}{\rho_w - \rho_p}$$

V — body volume in cm<sup>3</sup>,  $\Delta m$

— mass loss in g,  $\rho_w$  — distillate water density following Table 2 in g/cm<sup>3</sup>, and  $\rho_p$  — air density following Table 2 in g/cm<sup>3</sup>.

The numerical data obtained was statistically analyzed using the Statistica 12.5 software. The distribution of variables was assessed with the Shapiro–Wilk (W) test, while the homogeneity of variance was evaluated using Fisher's test. As the analyzed variables

followed a normal distribution, the results were presented as arithmetic means with standard deviations (SD). Mean comparisons were performed using Student's *t*-test for dependent (left–right) and independent (male–female) variables, as well as one-way analysis of variance (ANOVA). The developmental dynamics of the analyzed parameters were characterized using linear and nonlinear regression analysis. The fit of the estimated curves to the measurement data was assessed based on the coefficient of determination ( $R^2$ ). Differences were considered statistically significant at  $p < 0.05$ .

## RESULTS

The psoas major muscle was found in all specimens studied. Since the statistical analysis revealed neither sex nor bilateral differences for all the analyzed parameters ( $p > 0.05$ ), each parameter was aggregately presented for the whole group examined, without taking sex into account. The numerical findings of the psoas major have separately been tabularized for its length (Tab. 3), width (Tab. 4), projection surface area (Tab. 5) and volume (Tab. 6).

The mean total length of the psoas major at fetal ages 16–28 weeks grew from 30.06 to  $73.98 \pm 2.27$  mm on the right, and from 29.91 to  $72.76 \pm 1.77$  mm on the left, following the natural logarithmic function:  $y = -170.757 + 72.676 \times \ln(\text{age}) \pm 2.320$  ( $R^2 = 0.95$ ) — Figure 2A.

In fetuses aged 16–28 weeks, the mean belly length of the psoas major grew from 22.71 to  $52.21 \pm 3.78$  mm on the right, and from 21.18 to  $50.38 \pm 1.63$  mm on the left, in accordance with the third-degree polynomial function:  $y = 15.830 + 0.002 \times (\text{age})^3 \pm 2.141$  ( $R^2 = 0.91$ ) — Figure 2B.

Between weeks 16 and 28 of gestation, the mean tendon length of the psoas major increased from 7.35 mm to  $21.77 \pm 1.51$  mm on the right, and from 8.73 mm to  $22.39 \pm 0.13$  mm on the left, according to the natural logarithmic function:  $y = -52.490 + 22.924 \times \ln(\text{age}) \pm 1.818$  ( $R^2 = 0.76$ ) — Figure 2C.

During the study period, the mean distance from the muscle origin to the widest part of the muscle belly of the psoas major enlarged from 10.52 to  $25.32 \pm 0.65$  mm on the right, and from 7.48 to  $21.42 \pm 4.89$  mm on the left, and modelled the linear function:  $y = -4.752 + 0.984 \times \text{age} \pm 2.467$  ( $R^2 = 0.58$ ) — Figure 2D.

At the age of 16–28 weeks of gestation, the belly width of the psoas major measured at its widest level ranged from 4.26 to  $7.71 \pm 1.67$  mm on the right, and from 4.52 to  $8.82 \pm$

0.91 mm on the left, and computed the inverse function:  $y = 14.562 - 163.731/(\text{age}) \pm 0.626$  ( $R^2 = 0.76$ ) —Figure 2E.

In fetuses aged 16–28 weeks, the mean tendon width measured at its midway of the psoas major increased from 0.43 to  $2.10 \pm 0.06$  on the right, and from 0.55 to  $2.30 \pm 0.13$  mm on the left, and demonstrated the inverse function:  $y = 5.033 - 72.604/(\text{age}) \pm 0.215$  ( $R^2 = 0.84$ ) — Figure 2F.

During that time, the mean muscle projection surface area of the psoas major ranged from 62.16 to  $317.05 \pm 14.76$  mm<sup>2</sup> on the right, and from 59.69 to  $330.81 \pm 18.04$  mm<sup>2</sup> on the left, following the linear function:  $y = -312.843 + 23.285 \times \text{age} \pm 15.504$  ( $R^2 = 0.95$ ) — Figure 2G. The mean belly projection surface area of the psoas major grew from 57.80 to  $274.48 \pm 17.91$  mm<sup>2</sup> on the right, and from 56.74 to  $289.03 \pm 25.78$  mm<sup>2</sup> on the left, displaying the linear function:  $y = -264.233 + 19.761 \times \text{age} \pm 14.192$  ( $R^2 = 0.94$ ) — Figure 2H. The mean tendon projection surface area of the psoas major ranged from 4.36 to  $42.58 \pm 3.15$  mm<sup>2</sup> on the right, and from 2.95 to  $41.78 \pm 7.74$  mm<sup>2</sup> on the left, according to the linear function:  $y = -53.611 + 3.781 \times \text{age} \pm 5.217$  ( $R^2 = 0.83$ ) — Figure 2I.

At ages of 16–28 weeks of gestation, the mean muscle volume of the psoas major grew from 0.12 to  $1.29 \pm 0.25$  cm<sup>3</sup> on the right, and from 0.12 to  $1.32 \pm 0.20$  cm<sup>3</sup> on the left, in accordance with the linear function:  $y = -1.603 + 0.104 \times \text{age} \pm 0.105$  ( $R^2 = 0.89$ ) — Figure 3A.

The growth of the muscle belly and tendon (Fig. 3B, C) was expressed in a relative manner by the belly width-to-length ratio and tendon width-to-length ratio. The mean value of the belly width-to-length ratio decreased from  $0.20 \pm 0.03$  to  $0.16 \pm 0.02$ , while the mean value of the tendon width-to-length ratio increased from  $0.07 \pm 0.02$  to  $0.11 \pm 0.01$ .

As illustrated in Figures 3D and E, the mean value of the belly-to-muscle projection surface area ratio and tendon-to-muscle projection surface area ratio oscillated at the level  $0.85 \pm 0.04$  and  $0.15 \pm 0.04$ , respectively. As plotted in Figure 3F, the mean value of the tendon-to-belly projection surface area ratio gradually increased from  $0.15 \pm 0.05$  to  $0.18 \pm 0.04$ .

## DISCUSSION

Sex differences in skeletal muscles become noticeable as late as since 13 years of age, with more pronounced differences observed in the upper part of the body [13, 17, 29, 33]. Abe et al. [1] reported that sexual dimorphism in adult musculature is more pronounced in the torso compared to the limbs. Their study revealed that, at the level of the iliac crest, the cross-

sectional area of the psoas major muscle in women is only 61% of that in men. In turn, Marras et al. [20] found an even greater disparity, with the cross-sectional area of the psoas major muscle in women being just 54% of that in men. Cronin et al. [5] observed asymmetry of the psoas major, as the right muscle was bigger than the left one.

In the present study, however, no significant sex or bilateral differences were observed in the morphometry of the psoas major muscle. These findings align with those of Tanner et al. [33], Kanehisa et al. [17] and Hoshikawa et al. [13], who noted that sex differences in skeletal muscles size typically become apparent only during puberty. The absence of sexual dimorphism in the investigated muscles during fetal development is consistent with previous studies on the prenatal development of various skeletal muscles, including the palmaris longus [22], trapezius [18], semimembranosus [3], semitendinosus [4], deltoid [31], biceps brachii [32], triceps brachii [10] and quadratus lumborum [11].

In an autopsy study, Regev et al. [25] measured the length of the psoas major muscle from its origin to its insertion. The mean length of the muscle was reported to be  $27.42 \pm 2.1$  cm in women and  $31.96 \pm 4.1$  cm in men, with overall mean length of  $29.93 \pm 4$  cm for the entire study group. Based on only two cases, Friederich et al. [9] observed the psoas major to have a length of 24.8 cm. Similarly, Ward et al. [35] reported a mean length of  $24.25 \pm 4.75$  cm for this muscle.

In a study conducted by Santaguida and McGill [27], the mean length of the psoas major was found to be  $262 \pm 32$  mm, with the internal tendon measuring  $68 \pm 19$  mm and the external tendon measuring  $93 \pm 23$  mm. Using anatomical dissection, Spoor et al. [30] analyzed the psoas major muscle in a male newborn with a body length of 48 cm. Measurements were taken in two different body positions of the newborn: in the first position, the lower limbs were strongly flexed at the hips and knees, with the thighs externally rotated and slightly abducted, in the second position, referred to as the fetal position, the lower limbs were slightly flexed, abducted, and externally rotated. In the first position, the total length and cross-sectional area of the psoas major muscle were measured as 3.9 cm and  $1.08 \text{ cm}^2$ , respectively. In the fetal position, these values were 2.6 cm and  $1.62 \text{ cm}^2$ , respectively.

In the present study, we measured the psoas major muscles in fetuses with their lower limb extended, slightly adducted and externally rotated at the hip. The total length of the psoas major muscle and its tendon length increased logarithmically, in accordance with the functions:  $y = -170.757 + 72.676 \times \ln(\text{age}) \pm 2.3198$  and  $y = -52.4898 + 22.9240 \times \ln(\text{age}) \pm 1.8182$ , respectively. The belly length increased following the cubic function:  $y = 15.8304 + 0.0017 \times (\text{age})^3 \pm 2.1405$ . The developmental dynamics of the belly width and tendon width

increased in accordance with the regressions:  $y = 14.562 - 163.731/(\text{age}) \pm 0.6259$  and  $y = 5.0327 - 72.6035/(\text{age}) \pm 0.2146$ , respectively. The distance from the muscle origin to the widest part of the muscle belly followed the linear function:  $y = -4.752 + 0.984 \times \text{age} \pm 2.4673$ . In the material under examination, the belly width-to-length ratio decreased, indicating a relative elongation of the belly, while the tendon width-to-length ratio increased, indicating a faster growth of the tendon in width than in length.

The size of skeletal muscle, particularly its physiological cross-sectional area, is the most reliable indicator of muscle strength. Both age and sex significantly influence skeletal muscle size. Based on CT examinations, measurements of the cross-sectional area of the psoas major muscle revealed that its largest size occurs in men around 30 years of age. This size subsequently decreases, reaching approximately two-thirds of the baseline value by the age of 40 [15]. In women, the cross-sectional area of the psoas major muscle decreases to half of its baseline value by the age of 40 [15]. Among the muscles of the lower lumbar spine, the psoas major demonstrates the largest cross-sectional area. Numerous morphometric analyses of the cross-sectional area of the psoas major muscle have also been conducted using MRI [22–25].

In the material under examination, the muscle, belly and tendon projection surface areas increased proportionately to fetal age, following the functions:  $y = -312.843 + 23.285 \times \text{age} \pm 15.5036$ ;  $y = -264.233 + 19.761 \times \text{age} \pm 14.1923$  and  $y = -53.6106 + 3.7811 \times \text{age} \pm 5.2173$ , respectively.

To assess the relative planar proportions of the psoas major, the belly and tendon projection surface area ratios were calculated in this study. In the analyzed group, the belly-to-muscle projection surface area ratio represented on average  $85 \pm 4\%$ , while the tendon-to-muscle projection surface area ratio was on average  $15 \pm 4\%$ . In our study, we also calculated the tendon-to-belly projection surface area ratio of the psoas major. This index had been increasing in value up to 21–22 weeks of fetal age, and then stabilized at the level of  $0.17 \pm 0.06$ .

The present study revealed the volumetric growth of the psoas major to follow the following linear function  $y = -1.603 + 0.104 \times \text{age} \pm 0.105$ .

Unfortunately, no reports of the morphometric parameters of the psoas major muscle in human fetuses are available in the medical literature, which limits the ability to conduct a more detailed discussion on this topic.

Ultrasonography is the preferred imaging modality for assessing long bones, skeletal dysplasias and limb anomalies [27, 28]. However, it should be noted that ultrasound

evaluation of individual skeletal muscles can be highly challenging due to their indistinct separation from surrounding anatomical structures [22]. The psoas major muscle, in particular, poses imaging difficulties because of its deep anatomical location and frequent obscuration by intestinal gas [28]. Fortunately, magnetic resonance imaging (MRI) provides a reliable alternative, enabling precise visualization of the outlines and dimensions of individual muscles [22].

The numerical data for the psoas major obtained in the present study may prove valuable for assessing both the skeletal system and fetal development, with potential implications for surgical applications.

The main limitation of this study may be a relatively narrow gestational age range from 16 to 28 weeks and a small number of cases, comprising 67 human fetuses.

## **CONCLUSIONS**

1. The obtained numerical data of the psoas major muscle we considered age-specific reference values.
2. Neither sex nor bilateral differences are found for morphometric parameters of the psoas major.
3. In terms of morphometric parameters, the psoas major displays growth dynamics diverse to four functions: from a gradual inhibition of growth which is typical of both natural logarithmic functions (total muscle length and tendon length) and a reverse model (belly width and tendon width) through a linear growth (distance between the origin and the widest belly level, muscle projection surface area, belly projection surface area, tendon projection surface area and volume) to a hyperbolic growth (belly length).

## **ARTICLE INFORMATION AND DECLARATIONS**

### **Data availability statement**

Any additional data supporting this study are available from the corresponding author (M.G.) upon reasonable request.

### **Ethics statement**

This material has not been published in whole or in part elsewhere. The manuscript is not currently being considered for publication in another journal. The anatomical protocol of the study was accepted by the Bioethics Committee of Ludwik Rydygier Collegium Medicum in

Bydgoszcz (KB 124/2016). The fetuses were obtained from spontaneous abortions after parental consent and were from Department of Anatomy of Ludwik Rydygier Collegium Medicum of Nicolaus Copernicus. Everything was in accordance with the legal procedures in force in Poland and in accordance with the program Donation Corpse both adults and fetuses. This study was performed in line with the principles of the Declaration of Helsinki.

### **Author contributions**

**M.G.:** conceptualization, methodology, formal analysis, investigation, resources, data curation, writing — original draft preparation, writing — review and editing, visualization. **M.Sz.:** supervision, writing —review and editing. **M.K.:** methodology, investigation. **B.H.:** resources, data curation. **K.E.:** visualization. **M.B.:** formal analysis, supervision.

### **Funding**

This research did not receive any specific grant from funding agencies in the public, commercial, or not-for-profit sectors.

### **Acknowledgements**

The authors sincerely thank those who donated their bodies to science so that anatomical research could be performed. Results from such research can potentially increase mankind's overall knowledge that can then improve patient care. Therefore, these donors and their families deserve our highest gratitude [12, 36].

### **Conflict of interest**

The authors declare that they have no conflict of interest.

### **REFERENCES**

1. Abe T, Kearns CF, Fukunaga T. Sex differences in whole body skeletal muscle mass measured by magnetic resonance imaging and its distribution in young Japanese adults. *Br J Sports Med.* 2003; 37(5): 436–440, doi: [10.1136/bjism.37.5.436](https://doi.org/10.1136/bjism.37.5.436), indexed in Pubmed: [14514537](https://pubmed.ncbi.nlm.nih.gov/14514537/).
2. Arbanas J, Pavlovic I, Marijancic V, et al. MRI features of the psoas major muscle in patients with low back pain. *Eur Spine J.* 2013; 22(9): 1965–1971, doi: [10.1007/s00586-013-2749-x](https://doi.org/10.1007/s00586-013-2749-x), indexed in Pubmed: [23543369](https://pubmed.ncbi.nlm.nih.gov/23543369/).

3. Badura M, Wiśniewski M, Szpinda M, et al. Developmental dynamics of the semimembranosus muscle in human fetuses. *Med Biol Sci.* 2011; 25: 13–16.
4. Badura M, Wiśniewski M, Szpinda M, et al. The growth of the semitendinosus muscle in human fetuses. *Med Biol Sci.* 2011; 25: 17–21.
5. Cronin CG, Lohan DG, Meehan CP, et al. Anatomy, pathology, imaging and intervention of the iliopsoas muscle revisited. *Emerg Radiol.* 2008; 15(5): 295–310, doi: [10.1007/s10140-008-0703-8](https://doi.org/10.1007/s10140-008-0703-8), indexed in Pubmed: [18548299](https://pubmed.ncbi.nlm.nih.gov/18548299/).
6. Cutts A. Shrinkage of muscle fibres during the fixation of cadaveric tissue. *J Anat.* 1988; 160: 75–78, indexed in Pubmed: [3253263](https://pubmed.ncbi.nlm.nih.gov/3253263/).
7. Dangaria TR, Naesh O. Changes in cross-sectional area of psoas major muscle in unilateral sciatica caused by disc herniation. *Spine (Phila Pa 1976).* 1998; 23(8): 928–931, doi: [10.1097/00007632-199804150-00016](https://doi.org/10.1097/00007632-199804150-00016), indexed in Pubmed: [9580961](https://pubmed.ncbi.nlm.nih.gov/9580961/).
8. Danneels LA, Vanderstraeten GG, Cambier DC, et al. CT imaging of trunk muscles in chronic low back pain patients and healthy control subjects. *Eur Spine J.* 2000; 9(4): 266–272, doi: [10.1007/s005860000190](https://doi.org/10.1007/s005860000190), indexed in Pubmed: [11261613](https://pubmed.ncbi.nlm.nih.gov/11261613/).
9. Friederich JA, Brand RA. Muscle fiber architecture in the human lower limb. *J Biomech.* 1990; 23(1): 91–95, doi: [10.1016/0021-9290\(90\)90373-b](https://doi.org/10.1016/0021-9290(90)90373-b), indexed in Pubmed: [2307696](https://pubmed.ncbi.nlm.nih.gov/2307696/).
10. Grzonkowska M, Badura M, Lisiecki J, et al. Growth dynamics of the triceps brachii muscle in the human fetus. *Adv Clin Exp Med.* 2014; 23(2): 177–184, doi: [10.17219/acem/37045](https://doi.org/10.17219/acem/37045), indexed in Pubmed: [24913107](https://pubmed.ncbi.nlm.nih.gov/24913107/).
11. Grzonkowska M, Baumgart M, Badura M, et al. Quantitative anatomy of the growing quadratus lumborum in the human foetus. *Surg Radiol Anat.* 2018; 40(1): 91–98, doi: [10.1007/s00276-017-1901-4](https://doi.org/10.1007/s00276-017-1901-4), indexed in Pubmed: [28756538](https://pubmed.ncbi.nlm.nih.gov/28756538/).
12. Henry BM, Vikse J, Pekala P, et al. Consensus guidelines for the uniform reporting of study ethics in anatomical research within the framework of the anatomical quality assurance (AQUA) checklist. *Clin Anat.* 2018; 31(4): 521–524, doi: [10.1002/ca.23069](https://doi.org/10.1002/ca.23069), indexed in Pubmed: [29532521](https://pubmed.ncbi.nlm.nih.gov/29532521/).
13. Hoshikawa Y, Muramatsu M, Iida T, et al. Sex differences in the cross-sectional areas of psoas major and thigh muscles in high school track and field athletes and

- nonathletes. *J Physiol Anthropol.* 2011; 30(2): 47–53, doi: [10.2114/jpa2.30.47](https://doi.org/10.2114/jpa2.30.47), indexed in Pubmed: [21483176](https://pubmed.ncbi.nlm.nih.gov/21483176/).
14. Ilayperuma I, Nanayakkara BG. Gross anatomical characterization of the psoas major muscle: a cadaver study. *Galle Med J.* 2009; 13(1): 22, doi: [10.4038/gmj.v13i1.889](https://doi.org/10.4038/gmj.v13i1.889).
  15. Imamura K, Ashida H, Ishikawa T, et al. Human major psoas muscle and sacrospinalis muscle in relation to age: a study by computed tomography. *J Gerontol.* 1983; 38(6): 678–681, doi: [10.1093/geronj/38.6.678](https://doi.org/10.1093/geronj/38.6.678), indexed in Pubmed: [6630901](https://pubmed.ncbi.nlm.nih.gov/6630901/).
  16. Kamiya N, Zhou X, Chen H, et al. Automated segmentation of psoas major muscle in X-ray CT images by use of a shape model: preliminary study. *Radiol Phys Technol.* 2012; 5(1): 5–14, doi: [10.1007/s12194-011-0127-0](https://doi.org/10.1007/s12194-011-0127-0), indexed in Pubmed: [21755416](https://pubmed.ncbi.nlm.nih.gov/21755416/).
  17. Kanehisa H, Ikegawa S, Tsunoda N, et al. Cross-sectional areas of fat and muscle in limbs during growth and middle age. *Int J Sports Med.* 1994; 15(7): 420–425, doi: [10.1055/s-2007-1021081](https://doi.org/10.1055/s-2007-1021081), indexed in Pubmed: [8002122](https://pubmed.ncbi.nlm.nih.gov/8002122/).
  18. Kędzia A, Herlender M, Tomczyk M, et al. Musculus trapezius metrology in foetal period. *APM.* 2010; 16(3): 140–146.
  19. Mamatha H, Bhat K, Said O, et al. A comparative imaging analysis of paraspinal muscles in healthy individuals and patients with chronic low back pain. *Transl Res Anat.* 2024; 37: 100319, doi: [10.1016/j.tria.2024.100319](https://doi.org/10.1016/j.tria.2024.100319).
  20. Marras WS, Jorgensen MJ, Granata KP, et al. Female and male trunk geometry: size and prediction of the spine loading trunk muscles derived from MRI. *Clin Biomech (Bristol).* 2001; 16(1): 38–46, doi: [10.1016/s0268-0033\(00\)00046-2](https://doi.org/10.1016/s0268-0033(00)00046-2), indexed in Pubmed: [11114442](https://pubmed.ncbi.nlm.nih.gov/11114442/).
  21. Martin DC, Medri MK, Chow RS, et al. Comparing human skeletal muscle architectural parameters of cadavers with in vivo ultrasonographic measurements. *J Anat.* 2001; 199(Pt 4): 429–434, doi: [10.1046/j.1469-7580.2001.19940429.x](https://doi.org/10.1046/j.1469-7580.2001.19940429.x), indexed in Pubmed: [11693303](https://pubmed.ncbi.nlm.nih.gov/11693303/).
  22. Nemec SF, Nemec U, Brugger PC, et al. MR imaging of the fetal musculoskeletal system. *Prenat Diagn.* 2012; 32(3): 205–213, doi: [10.1002/pd.2914](https://doi.org/10.1002/pd.2914), indexed in Pubmed: [22430716](https://pubmed.ncbi.nlm.nih.gov/22430716/).

23. Peltonen JE, Taimela S, Erkinntalo M, et al. Back extensor and psoas muscle cross-sectional area, prior physical training, and trunk muscle strength--a longitudinal study in adolescent girls. *Eur J Appl Physiol Occup Physiol*. 1998; 77(1-2): 66–71, doi: [10.1007/s004210050301](https://doi.org/10.1007/s004210050301), indexed in Pubmed: [9459523](https://pubmed.ncbi.nlm.nih.gov/9459523/).
24. Ploumis A, Michailidis N, Christodoulou P, et al. Ipsilateral atrophy of paraspinal and psoas muscle in unilateral back pain patients with monosegmental degenerative disc disease. *Br J Radiol*. 2011; 84(1004): 709–713, doi: [10.1259/bjr/58136533](https://doi.org/10.1259/bjr/58136533), indexed in Pubmed: [21081573](https://pubmed.ncbi.nlm.nih.gov/21081573/).
25. Regev GJ, Kim CW, Tomiya A, et al. Psoas muscle architectural design, in vivo sarcomere length range, and passive tensile properties support its role as a lumbar spine stabilizer. *Spine (Phila Pa 1976)*. 2011; 36(26): E1666–E1674, doi: [10.1097/BRS.0b013e31821847b3](https://doi.org/10.1097/BRS.0b013e31821847b3), indexed in Pubmed: [21415810](https://pubmed.ncbi.nlm.nih.gov/21415810/).
26. Sajko S, Stuber K. Psoas major: a case report and review of its anatomy, biomechanics, and clinical implications. *J Can Chiropr Assoc*. 2009; 53(4): 311–318.
27. Santaguida PL, McGill SM. The psoas major muscle: a three-dimensional geometric study. *J Biomech*. 1995; 28(3): 339–345, doi: [10.1016/0021-9290\(94\)00064-b](https://doi.org/10.1016/0021-9290(94)00064-b), indexed in Pubmed: [7730392](https://pubmed.ncbi.nlm.nih.gov/7730392/).
28. Smereczyński A, Bojko S, Gałdyńska M, et al. Mięsień biodrowo-lędźwiowy. Część 1. Metodyka badania i anatomia ultrasonograficzna. *Ultrasonografia*. 2007; 31: 61–67.
29. Snow EL. Variation is the rule: Insights about translational research on anatomical variations. *Transl Res Anat*. 2024; 37: 100333, doi: [10.1016/j.tria.2024.100333](https://doi.org/10.1016/j.tria.2024.100333).
30. Spoor CW, van Leeuwen JL, de Windt FH, et al. A model study of muscle forces and joint-force direction in normal and dysplastic neonatal hips. *J Biomech*. 1989; 22(8-9): 873–884, doi: [10.1016/0021-9290\(89\)90071-7](https://doi.org/10.1016/0021-9290(89)90071-7), indexed in Pubmed: [2613723](https://pubmed.ncbi.nlm.nih.gov/2613723/).
31. Szpinda M, Paruszevska–Achtel M, Baumgart M, et al. Quantitative growth of the human deltoid muscle in human fetuses. *Med Biol Sci*. 2011; 25(3): 59–64.
32. Szpinda M, Paruszevska-Achtel M, Dąbrowska M, et al. The normal growth of the biceps brachii muscle in human fetuses. *Adv Clin Exp Med*. 2013; 22(1): 17–26, indexed in Pubmed: [23468258](https://pubmed.ncbi.nlm.nih.gov/23468258/).

33. Tanner JM, Hughes PC, Whitehouse RH. Radiographically determined widths of bone muscle and fat in the upper arm and calf from age 3-18 years. *Ann Hum Biol.* 1981; 8(6): 495–517, doi: [10.1080/03014468100005351](https://doi.org/10.1080/03014468100005351), indexed in Pubmed: [7337414](https://pubmed.ncbi.nlm.nih.gov/7337414/).
34. Tufo A, Desai GJ, Cox WJ. Psoas syndrome: a frequently missed diagnosis. *J Am Osteopath Assoc.* 2012; 112(8): 522–528, doi: [10.7556/jaoa.2012.112.8.522](https://doi.org/10.7556/jaoa.2012.112.8.522), indexed in Pubmed: [22904251](https://pubmed.ncbi.nlm.nih.gov/22904251/).
35. Ward SR, Eng CM, Smallwood LH, et al. Are current measurements of lower extremity muscle architecture accurate? *Clin Orthop Relat Res.* 2009; 467(4): 1074–1082, doi: [10.1007/s11999-008-0594-8](https://doi.org/10.1007/s11999-008-0594-8), indexed in Pubmed: [18972175](https://pubmed.ncbi.nlm.nih.gov/18972175/).
36. Wysiadecki G, Varga I, Klejbor I, et al. Reporting anatomical variations: Should unified standards and protocol (checklist) for anatomical studies and case reports be established? *Transl Res Anat.* 2024; 35: 100284, doi: [10.1016/j.tria.2024.100284](https://doi.org/10.1016/j.tria.2024.100284).
37. Yasar S, Kaya S, Temiz C, et al. Morphological structure and variations of lumbar plexus in human fetuses. *Clin Anat.* 2014; 27(3): 383–388, doi: [10.1002/ca.22111](https://doi.org/10.1002/ca.22111), indexed in Pubmed: [22696243](https://pubmed.ncbi.nlm.nih.gov/22696243/).
38. Yoshio M, Murakami G, Sato T, et al. The function of the psoas major muscle: passive kinetics and morphological studies using donated cadavers. *J Orthop Sci.* 2002; 7(2): 199–207, doi: [10.1007/s007760200034](https://doi.org/10.1007/s007760200034), indexed in Pubmed: [11956980](https://pubmed.ncbi.nlm.nih.gov/11956980/).

**Table 1** Age, number and sex of the fetuses studied.

Gestational age	Crown-rump length [mm]				Number		
					of	Sex	
Weeks (Hbd-life)	Mean	SD	Min.	Max.	fetuses		
					N	♂	♀
16	101		101	101	1	1	
17	118	5.00	113	123	3	2	1
18	131.08	3.70	125	136	12	6	6
19	143.43	3.51	139	150	7	4	3
20	156.86	3.63	152	160	7	2	5
21	170.55	2.88	165	174	11	4	7
22	180.50	2.59	176	183	6	2	4
23	188.00		188	188	1	1	
24	203.14	2.91	200	208	7	3	4

25	213.20	3.19	211	218	5	4	1
26	224.50	6.36	220	229	2	1	1
27	234	1.73	232	235	3	1	2
28	240		240	240	2		2
Total					67	31	36

Hbd. — human biocultural development; Max — maximum; Min — minimum; SD — standard deviation.

**Table 2.** Destillate water and air density for temperature 19–28°C.

Temperature [°C]	Water	Air
	density [g/cm <sup>3</sup> ]	density [g/cm <sup>3</sup> ]
19	0.9984	0.0012
		2
20	0.9982	0.0012
		2
21	0.9979	0.0012
	9	1
22	0.9977	0.0012
	7	1
23	0.9975	0.0012
	4	
24	0.9973	0.0012
	0.9970	
25		0.0012
	5	
26	0.9967	0.0011
	9	9
27	0.9965	0.0011
	3	9
28	0.9962	0.0011
	5	8

**Table 3.** Total length, belly length and tendon length of the psoas major muscle.

Gestational age [weeks]	Number of fetuses	Total length [mm]					Belly length [mm]					Tendon length [mm]				
		Right		Left			Right		Left			Right		Left		
		Mean	SD	Mean	SD	P	Mean	SD	Mean	SD	P	Mean	SD	Mean	SD	P
16	1	30.06		29.91		≤ 0.05	22.71		21.18		≤ 0.05	7.35		8.73		≤ 0.05
17	3	33.32	0.49	32.12	2	≤ 0.05	21.97	1.39	22.06	1.87	≤ 0.05	11.35	0.91	10.06	0.85	≤ 0.05
18	12	37.76	1.75	37.36	1.99	≤ 0.05	25.01	2.22	24.81	2.45	≤ 0.05	12.76	1.1	12.55	1.45	≤ 0.05
19	7	42.89	2.41	42.37	2.06	≤ 0.05	28.04	1.78	26.89	1.21	≤ 0.05	14.85	1.22	15.48	1.86	≤ 0.05
20	7	45.05	3.53	45.53	2.84	≤ 0.05	29.26	2.3	29.75	1.67	≤ 0.05	15.8	1.54	15.78	1.78	≤ 0.05
21	11	49.06	1.3	49.99	2.78	≤ 0.05	30.73	1.99	31.23	1.62	≤ 0.05	18.32	2.48	18.76	2.53	≤ 0.05
22	6	50.76	1.72	51.36	1.53	≤ 0.05	31.25	1.86	31.4	1.59	≤ 0.05	19.51	1.29	19.96	0.42	≤ 0.05
23	1	50.7		49.99		≤ 0.05	33.33		31.62		≤ 0.05	17.37		18.37		≤ 0.05
24	7	57.76	1.39	58.29	1.13	≤ 0.05	38.63	1.95	39.73	1.69	≤ 0.05	19.13	1.01	18.56	2.33	≤ 0.05
25	5	60	2.53	60.6	2.7	≤ 0.05	39.44	2.7	39.37	3.32	≤ 0.05	20.56	3.02	21.23	1.7	≤ 0.05
26	2	62.64	1.81	62.29	1.99	≤ 0.05	45.51	1.78	41.87	1.51	≤ 0.05	17.13	0.03	20.42	0.48	≤ 0.05
27	3	68.68	2.28	70.06	1.68	≤ 0.05	45.84	2.56	47.3	2.91	≤ 0.05	22.84	2.16	22.76	1.74	≤ 0.05
28	2	73.98	2.27	72.76	1.77	≤ 0.05	52.21	3.78	50.38	1.63	≤ 0.05	21.77	1.51	22.39	0.13	≤ 0.05

SD — standard deviation.



**Table 4.** Belly width, distance between the muscle origin and the widest part of the muscle belly and tendon width of the psoas major muscle.

Gestational age [weeks]	Number of fetuses	Belly width [mm]					Distance between the muscle origin and the widest part of the muscle belly [mm]						Tendon width [mm]			
		Right		Left		P	Right		Left		P	Right		Left		P
		Mean	SD	Mean	SD		Mean	SD	Mean	SD		Mean	SD			
16	1	4.26		4.52		≤ 0.05	10.52		7.48		≤ 0.05	0.43		0.55		≤ 0.05
17	3	4.1	0.82	4.27	0.56	≤ 0.05	13.16	2.56	11.42	1.79	≤ 0.05	0.89	0.11	0.54	0.12	≤ 0.05
18	12	5.09	0.62	5.11	0.87	≤ 0.05	12.63	2.06	12.97	2.92	≤ 0.05	0.93	0.25	1	0.21	≤ 0.05
19	7	5.87	0.89	5.96	0.54	≤ 0.05	12.6	2.29	11.24	2.27	≤ 0.05	0.87	0.21	1.06	0.12	≤ 0.05
20	7	6.66	0.85	6.74	0.67	≤ 0.05	14.22	2.09	14.89	1.88	≤ 0.05	1.19	0.27	1.28	0.2	≤ 0.05
21	11	6.43	0.51	6.51	0.46	≤ 0.05	17.23	2.95	16.04	2.33	≤ 0.05	1.64	0.24	1.55	0.16	≤ 0.05
22	6	7.34	0.42	7.45	0.85	≤ 0.05	16.15	2.95	17.21	2.27	≤ 0.05	1.71	0.12	1.76	0.11	≤ 0.05
23	1	7.47		7.45		≤ 0.05	14.86		17.48		≤ 0.05	1.79		1.68		≤ 0.05
24	7	7.68	0.39	7.53	0.66	≤ 0.05	18.15	1.12	19.23	3.79	≤ 0.05	1.94	0.29	2.07	0.31	≤ 0.05
25	5	7.78	0.81	7.79	0.4	≤ 0.05	18.63	2.67	16.81	1.46	≤ 0.05	2.2	0.37	2.33	0.36	≤ 0.05

26	2	7.59	1.11	8.45	0.25	$\leq$ 0.05	21.65	5.11	19.06	0.69	$\leq 0.05$	1.81	0.13	2.29	0.73	$\leq 0.05$
27	3	8.13	0.26	7.32	0.23	$\leq$ 0.05	19.39	2.5	25.49	2.08	$\leq 0.05$	2.59	0.06	2.44	0.37	$\leq 0.05$
28	2	7.71	1.67	8.82	0.91	$\leq$ 0.05	25.32	0.65	21.42	4.89	$\leq 0.05$	2.1	0.06	2.3	0.13	$< 0.05$

---

SD — standard deviation.

**Table 5.** Muscle projection surface area, belly projection surface area and tendon projection surface area of the psoas major muscle.

Gestational age [weeks]	Number of fetuses	Muscle projection surface area [mm <sup>2</sup> ]					Belly projection surface area [mm <sup>2</sup> ]					Tendon projection surface area [mm <sup>2</sup> ]				
		Right		Left		P	Right		Left		P	Right		Left		P
		Mean	SD	Mean	SD		Mean	SD	Mean	SD		Mean	SD	Mean	SD	
16	1	62.16		59.69		≤ 0.05	57.8		56.74		≤ 0.05	4.36		2.95		≤ 0.05
17	3	69.16	4.72	71.05	5.91	≤ 0.05	57.18	7.83	62.83	5.68	≤ 0.05	11.98	4.04	8.22	2.92	≤ 0.05
18	12	98.16	14.96	96.64	19.04	≤ 0.05	85.27	13.22	84.19	17.76	≤ 0.05	12.89	2.43	12.45	2.31	≤ 0.05
19	7	119.41	14.49	121.44	9.71	≤ 0.05	105.38	15.24	104.85	7.96	≤ 0.05	14.03	4.72	16.6	3.3	≤ 0.05
20	7	140.59	11.69	143.1	7.82	≤ 0.05	122.74	11.27	122.67	8.7	≤ 0.05	17.85	4.1	20.43	3.13	≤ 0.05
21	11	163.17	11.92	169.69	12.95	≤ 0.05	136.65	17.06	140.97	14.13	≤ 0.05	26.52	8.64	28.72	8.67	≤ 0.05
22	6	185.08	22.11	192.34	31.38	≤ 0.05	154.4	16.85	161.58	23.61	≤ 0.05	30.68	7.05	30.76	8.15	≤ 0.05
23	1	174.09		181.65		≤ 0.05	146.93		153.09		≤ 0.05	27.16		28.56		≤ 0.05
24	7	236.34	13.21	252.37	26.59	≤ 0.05	198.37	10.12	215.32	24.2	≤ 0.05	37.96	8.45	37.04	8.38	≤ 0.05
25	5	248.06	38.32	258.74	25.19	≤ 0.05	211.64	32.86	216.21	20.56	≤ 0.05	36.42	7.71	42.53	6.52	≤ 0.05
26	2	263.57	19.26	286.8	0.55	≤ 0.05	229.94	10.96	242.54	11.43	≤ 0.05	33.63	8.3	44.26	11.98	≤ 0.05
27	3	314.26	20.15	300.39	36.03	≤ 0.05	266.64	18.09	249.78	41.54	≤ 0.05	47.62	2.52	50.61	6.71	≤ 0.05
28	2	317.05	14.76	330.81	18.04	≤ 0.05	274.48	17.91	289.03	25.78	≤ 0.05	42.58	3.15	41.78	7.74	≤ 0.05

SD — standard deviation.

**Table 6.** Volume of the psoas major muscle.

Gestation [weeks]	Number of fetuses	Volume [cm <sup>3</sup> ]		P
		Right	Left	
16	1	0.12	0.12	≤ 0.05
17	3	0.15	0.14	≤ 0.05
18	12	0.24	0.23	≤ 0.05
19	7	0.32	0.31	≤ 0.05
20	7	0.44	0.44	≤ 0.05
21	11	0.54	0.49	≤ 0.05
22	6	0.66	0.64	≤ 0.05
23	1	0.63	0.69	≤ 0.05
24	7	0.88	0.88	≤ 0.05
25	5	0.98	0.86	≤ 0.05
26	2	1.09	1.08	≤ 0.05
27	3	1.08	0.99	≤ 0.05
28	2	1.29	1.32	≤ 0.05

SD — standard deviation.

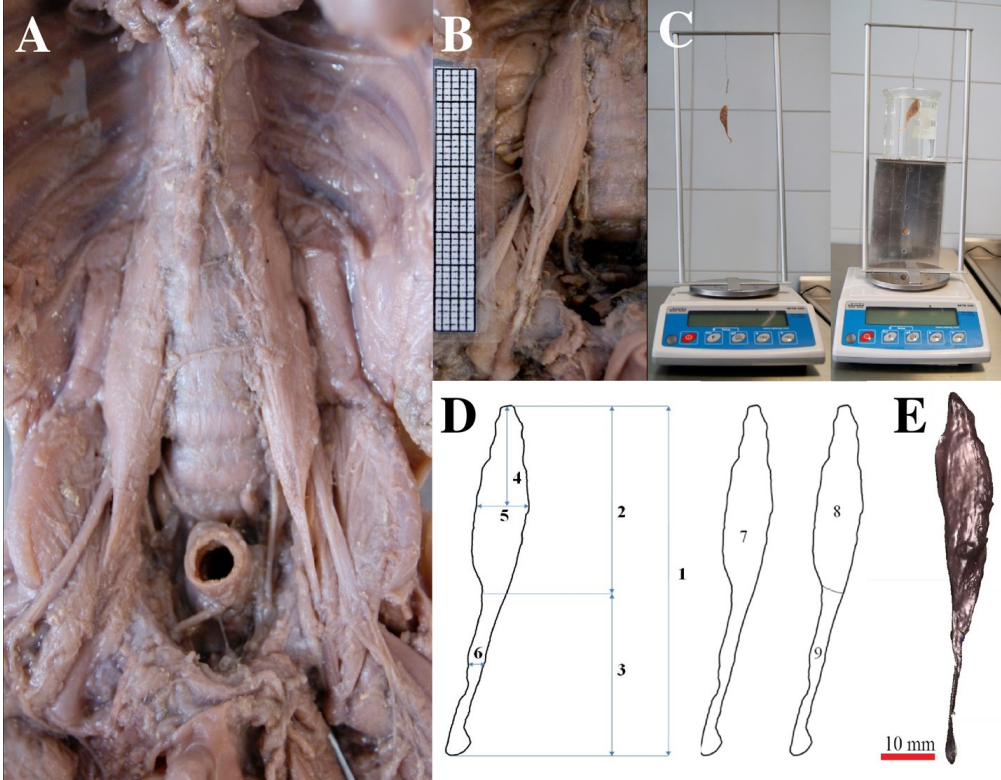


**Figure 1.** The psoas major muscle in a male (A) and female (B) fetus at 24 weeks, the hydrostatic method (C), measured parameters (D): 1 — total length, 2 — belly length, 3 — tendon length, 4 — distance between the muscle origin and the widest part of the muscle belly, 5 — belly width, 6 — tendon width, 7 — muscle projection surface area, 8 — belly projection surface area, 9 — tendon projection surface area, and 3D reconstruction (E).

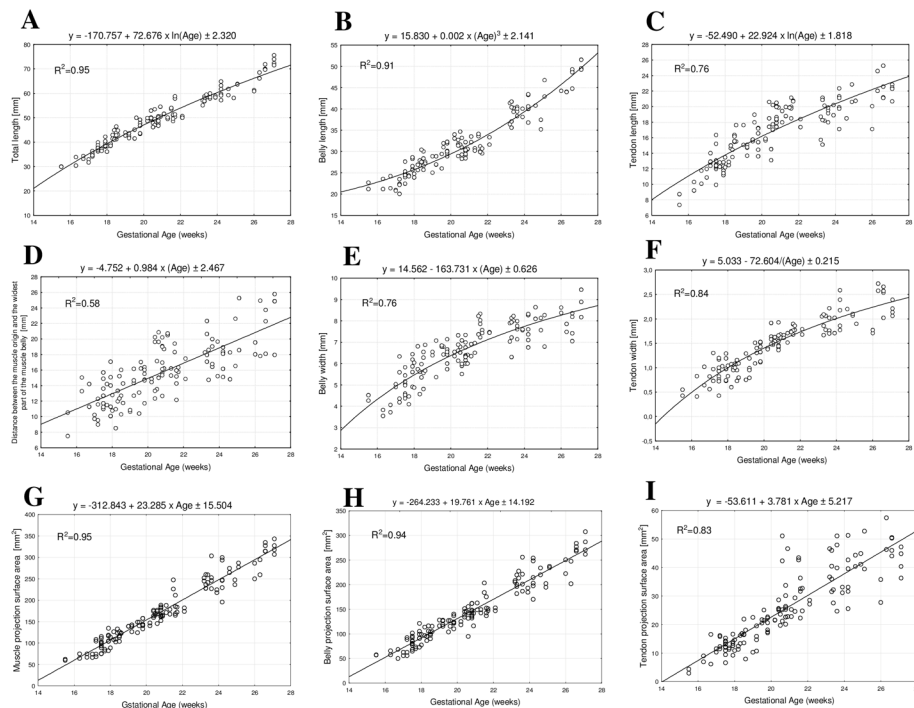


**Figure 2.** Regression lines for total length (A), belly length (B), tendon length (C) and distance between the muscle origin and the widest part of the muscle belly (D), belly width (E), tendon width (F), muscle projection surface area (G), belly projection surface area (H) and tendon projection surface area (I) of the psoas major muscle.

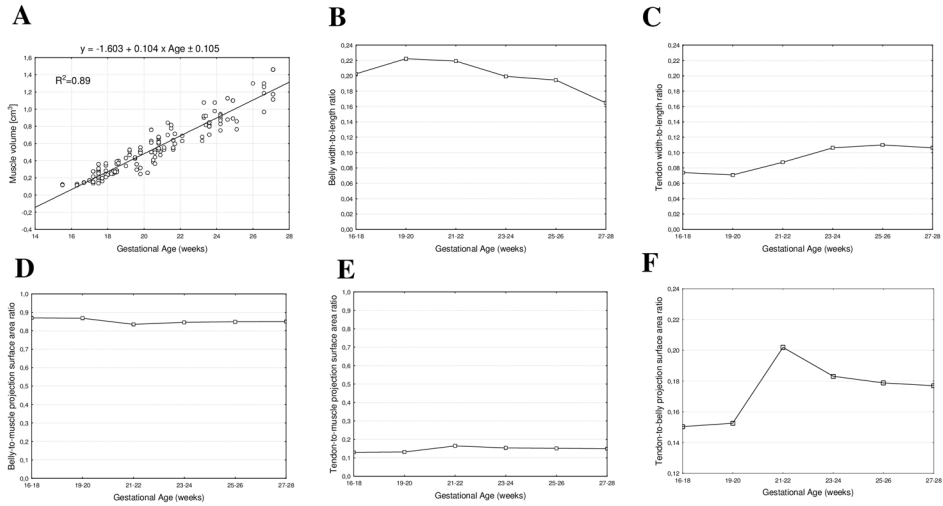


**Figure 3.** Regression line for volume (**A**) and charts for muscle belly width-to-length ratio (**B**), tendon width-to-length ratio (**C**), belly-to-muscle projection surface area ratio (**D**), tendon-to-muscle projection surface area ratio (**E**), tendon-to-belly projection surface area ratio (**F**) of the psoas major.